Toward Understanding the Nature of Internal Rotation Barriers with a New Energy Partition Scheme: Ethane and *n*-Butane

Shubin Liu*,† and Niranjan Govind‡

Renaissance Computing Institute, University of North Carolina, Chapel Hill, North Carolina 27599-3455, and William R. Wiley Environmental Molecular Sciences Laboratory, Pacific Northwest National Laboratory, Richland, Washington 99352

Received: January 15, 2008; Revised Manuscript Received: April 29, 2008

On the basis of an alternative energy partition scheme where density-based quantification of the steric effect was proposed [Liu, S. B. *J. Chem. Phys.* **2007**, *126*, 244103], the origin of the internal rotation barrier between the eclipsed and staggered conformers of ethane and n-butane is systematically investigated in this work. Within the new scheme, the total electronic energy is decomposed into three independent components, steric, electrostatic, and fermionic quantum. The steric energy defined in this way is repulsive, exclusive, and extensive and intrinsically linked to Bader's atoms in molecules approach. Two kinds of differences, adiabatic (with optimal structure) and vertical (with fixed geometry), are considered for the molecules in this work. We find that in the adiabatic case the eclipsed conformer possesses a larger steric repulsion than the staggered conformer for both molecules, but in the vertical cases the staggered conformer retains a larger steric repulsion. For ethane, a linear relationship between the total energy difference and the fermionic quantum energy difference is discovered. This linear relationship, however, does not hold for *n*-butane, whose behaviors in energy component differences are found to be more complicated. The impact of basis set and density functional choices on energy components from the new energy partition scheme has been investigated, as has its comparison with another definition of the steric effect in the literature in terms of the natural bond orbital analysis through the Pauli Exclusion Principle. In addition, profiles of conceptual density functional theory reactivity indices as a function of dihedral angle changes have been examined. Put together, these results suggest that the new energy partition scheme provides insights from a different perspective of internal rotation barriers.

I. Introduction

Computing hardware and software have progressed tremendously in the past decades, and computational chemistry has been becoming one of the most important disciplines in chemistry. Accurate predictions of structural, spectroscopic, and reactivity properties for small- to medium-sized molecular systems have become routinely accessible. Nevertheless, there still exists great controversy over the origin of the internal rotational barrier even for as simple a molecule as ethane or *n*-butane.[1–29] With modern computational chemistry approaches, one can very accurately calculate the internal rotational barrier height for these molecules. Indeed, faithful estimations of the barrier height for ethane and others were made more than 70 years ago.[1] Systematic improvements and possible explanations have consistently been the interest in the literature.[2–17] A number of different interpretations on the origin of the barrier have been available.[2,13,15,18,23,25] However, no consensus has been in place,[22–25] and the debate will likely keep on.[26–29] On the other hand, an unambiguous understanding is vitally significant in our knowledge to fathom molecular conformation changes, which are closely related to such prominent problems in chemistry and biology as protein folding, signal transduction, as well as chemical reactivity involving regio-, diastereo-, and enantioselectivity.

The controversy mainly lies in the answer to the question of where the barrier height comes from.[21–29] In central debate is the different amount of contributions from steric, electrostatic, and hyperconjugation (quantum) effects to the barrier height. The controversy, taking ethane as an example, is often characterized by two extreme explanations, one by Mulliken[2] suggesting that the hyperconjugation effect from the vicinal interactions between occupied σ_{CH} bond orbitals of one methyl group and virtual antibonding σ_{CH}* orbitals of the other methyl group plays the dominant role and the other by the intuitive, steric repulsion theory dictating that the barrier originates from the greater steric repulsion in the eclipsed isomer due to electrostatic and Pauli exchange interactions.[13,16] Different implementations of the above ideas using the orthogonal or nonorthogonal localized molecular orbital, natural bond orbital, and valence-bond orbital are available,[16,23,25,29] resulting in subtle but different explanations and thus ongoing debate in the literature.

Taking a closer look, we notice that the dispute was exclusively based on the definition of steric and hyperconjugations (quantum) effects from the wave function theory. Is there any density-based counterpart for them? Also, chemical concepts employed in the explanation such as steric effect are *noumena*,[30–32] objects of human inquiry, understanding or cognition, in contrast with *phenomena*. Though chemically significant and conceptually relevant in understanding the behavior of molecules, noumena are of purely rational apprehension and intellectual intuition and are not physically observable. In this regard,

* To whom correspondence should be addressed.
† University of North Carolina.
‡ Pacific Northwest National Laboratory.

10.1021/jp800376a CCC: $40.75
Published on Web 06/19/2008

quantum mechanically speaking, there is no unique description for them. Taking the steric effect as an example, according to Weisskopf,[33] it results from the "kinetic energy pressure" in atoms and molecules. Later, the concept was attributed to the quantum contribution[34] from the Pauli Exclusion Principle (Fermi hole),[35] and different implementations have been available in the literature.[23,25,29,34] In principle, however, this effect originates from the fact that atoms in molecules occupy a certain amount of space. When atoms are brought together, hindrance will be induced, resulting in changes in shape, energy, reactivity, etc. So, it is our view that the disagreement more likely comes from the different understanding and disparate attribution of noumena like steric effect.

In this work, the origin of the internal rotation barrier between the eclipsed and staggered conformers of ethane and *n*-butane is systematically investigated from a completely different perspective, using an alternative energy partition scheme where density-based quantification of the steric and quantum effects have previously been proposed.[36] Within the new scheme under the framework of density functional theory, the total energy density functional is assumed to be decomposed into three independent contributions from steric, electrostatic, and quantum effects, respectively. Attractive properties of the new definition have been revealed, and its intrinsic relation to Bader's atoms in molecules[37] approach has been discussed. In this work, we apply the idea to ethane and *n*-butane to examine the relative contributions of the three energy components during internal molecular rotations, providing insights for the understanding of the origin of molecular internal rotation barriers from a different perspective.

II. Theoretical Framework

Understanding the steric effect is critical to chemistry, biochemistry, and pharmacology as the effect is nearly universal, affecting the rates and energies of most chemical reactions, influencing the structure, dynamics, and function of naturally occurring molecules such as enzymes, and determining how and at what rate a drug will interact with its target biomolecules.

In ref 36, one of the authors recently proposed a new energy partition scheme within the framework of density functional theory, assuming that the total electronic energy density functional of an atom and molecular system can alternatively be decomposed into three *independent* contributions

$$E[\rho] \equiv E_s[\rho] + E_e[\rho] + E_q[\rho] \quad (1)$$

where $E_s[\rho]$, $E_e[\rho]$, and $E_q[\rho]$ stand for the energy components for the steric, electrostatic, and quantum effects, respectively. We reiterate that eq 1 is a hypothesis because the independence of the three functionals on the right-hand side is conjectured.

In DFT,[38] we know that

$$E[\rho] = T_s[\rho] + V_{ne}[\rho] + J[\rho] + E_{xc}[\rho] \quad (2)$$

where $T_S[\rho]$, $V_{ne}[\rho]$, $J[\rho]$, and $E_{xc}[\rho]$ represent the noninteracting kinetic, nuclear-electron attraction, classical electron−electron Coulomb repulsion, and exchange-correlation energy density functionals, respectively. Two terms in eq 2, $V_{ne}[\rho]$ and $J[\rho]$, are of the electrostatic nature. Hence

$$E_e[\rho] = V_{ne}[\rho] + J[\rho] \quad (3)$$

When computing the total energy of the system, one needs add another term, the nuclear−nuclear repulsion V_{nn}, which is also of electrostatic nature, into E_e[36] For the quantum contribution, one has

$$E_q[\rho] = E_{xc}[\rho] + E_{Pauli}[\rho] = E_{xc}[\rho] + T_s[\rho] - T_w[\rho] \quad (4)$$

where the Pauli energy[39–43] is

$$E_{Pauli}[\rho] \equiv T_s[\rho] - T_w[\rho] \quad (5)$$

denoting the portion of the kinetic energy that embodies all the effect from the antisymmetric requirement of the total wave function by the Pauli Exclusion Principle. $T_w[\rho]$ is the Weizsäcker kinetic energy[44]

$$T_w[\rho] = \frac{1}{8}\int \frac{|\nabla \rho(\mathbf{r})|^2}{\rho(\mathbf{r})} d\mathbf{r} \quad (6)$$

With eqs 1–4, there comes our density-based quantification of the steric energy

$$E_s[\rho] \equiv E[\rho] - E_e[\rho] - E_q[\rho] = T_w[\rho] \quad (7)$$

The physical meaning of the above definition is as follows. One uses the boson state as the reference, hypothesizing that if electrons were bosons, all electrons in the ground -state would be in the lowest orbital and the total energy of the state without considering the contributions from electrostatic and quantum effects would simply be $E_s[\rho]$. It represents the minimal space withheld by the state, and $E_s[\rho]$ is hence an intrinsic property of the system. This definition is consistent with the original Weisskopf's attribution[33] of the steric effect to the "kinetic energy pressure" because $T_w[\rho]$ itself is indeed a kinetic energy, exact for one electron systems. One notices that Nagy[45] recently linked the current description of the steric effect to the Fisher information and suggested to call the quantum effect as the fermionic quantum effect because the conjectured boson state is used as the reference state. The potential associating with the three exclusive contributions, steric, electrostatic, and quantum, can be respectively defined as the functional derivative of the energy component with respect to the total electron density.[36]

A few appealing characteristics with this definition have also been revealed.[36] First, it is repulsive, since the integrant of eq 6 is nowhere negative. Second, it is extensive because E_s is homogeneous of degree 1 in density scaling, $E_s[\gamma\rho] = \gamma E_s[\rho]$, for $0 \le \gamma \le 1$. Another property of the definition is its exclusiveness, i.e., independence of other quantities, as the assumption in eq 1. Also, we noticed that in the limit of homogeneous electron gas where the density gradient vanishes, the steric effect also disappears. For one-electron cases such as H and H_2^+ in their equilibrium geometry one has $E = -E_s$. More importantly, when we adopt Bader's zero flux condition[37] of atoms in molecules, where the zero flux surfaces S of the electron density $\rho(\mathbf{r})$ are defined as the set of points, **r,** obeying

$$\nabla \rho(\mathrm{r})\mathbf{n}(\mathrm{r}) = 0 \; \forall \; \mathrm{r} \in \mathrm{S} \quad (8)$$

where $\mathbf{n}(\mathbf{r})$ is the unit vector perpendicular to S at $\mathbf{r}$, the concept of atoms in molecules can then be established with the characteristic that the atoms are interfaced with each other with a vanished steric energy density surface, exhibiting that atoms in a molecule acquire balanced steric repulsion among one another. With the adoption of Bader's concept of atoms in molecules, one can quantify the energy components in eq 1 at both atomic and group resolutions.

As a manifestation and verification of the argument that such a noumenon as the steric effect cannot uniquely be defined, in a recent work,[46] we have showed that for atoms and molecules there exist two equivalent expressions for the Fisher information,[47] since

$$\int \frac{\nabla\rho(\mathbf{r}) \cdot \nabla\rho(\mathbf{r})}{\rho(\mathbf{r})} d\mathbf{r} = \int \nabla\rho(\mathbf{r}) \cdot \nabla \ln \rho(\mathbf{r}) d\mathbf{r}$$

$$= -\int \nabla^2\rho(\mathbf{r}) \ln \rho(\mathbf{r}) d\mathbf{r} \quad (9)$$

Notice the intrinsic relationship between the Fisher information, the first integral above, and the Weizsäcker kinetic energy, eq 6, and thus the steric energy.[45] For atoms and molecules, three integrals in eq 9 are identities, generating the same value for the integrals, but their local behaviors are markedly different as showcased elsewhere.[46,48]

There is another quantitative description of the steric effect in the literature in terms of the Pauli Exclusion Principle (Fermi hole). Since it is wave function based, different implementations using the orthogonal or nonorthogonal localized molecular orbital, natural bond orbital, or valence-bond orbital are available.[23,25,29,37] Notice that there is a fundamental difference between these two quantitative descriptions of the steric effect. In our present approach, we assumed the validity of the exclusiveness hypothesis of the total energy partition, eq 1, and categorically included all contributions from the Pauli Exclusion Principle into the fermionic quantum effect. In this work, besides providing insights about the origin of the rotational barrier heights for the two systems from the perspective of the new energy partition, we will also make brief comparison between the two descriptions of the steric effect.

Density functional theory (DFT) reactivity indices are conceptually insightful and practically convenient in predicting chemical reactivity of molecules.[49] We anticipate that they are equally important in understanding conformational changes.[50–54] In DFT,[38] the chemical potential, μ, and chemical hardness, η, are defined as

$$\mu = -\chi = \left(\frac{\partial E}{\partial N}\right)_v \quad (10)$$

and

$$\eta = \left(\frac{\partial^2 E}{\partial N^2}\right)_v = \left(\frac{\partial \mu}{\partial N}\right)_v \quad (11)$$

where E is the total energy of the system, N is the number of electrons in the system, and v is the external potential. μ is identified as the negative of electronegativity (χ).[55] According to Mulliken,[56] one has

$$\mu = -\chi = -\frac{1}{2}(I + A) \quad (12)$$

and according to Parr and Pearson[57]

$$\eta = I - A \quad (13)$$

where I and A are the first ionization potential and electron affinity, respectively. Under the Koopmans' theorem for closed-shell molecules, based on the finite difference approach, I and A can be expressed in terms of the highest occupied molecular orbital (HOMO) energy, $\varepsilon_{\mathrm{HOMO}}$, and the lowest unoccupied molecular orbital (LUMO) energy, $\varepsilon_{\mathrm{LUMO}}$, respectively

$$I \approx -\varepsilon_{\mathrm{HOMO}} \qquad A \approx -\varepsilon_{\mathrm{LUMO}} \quad (14)$$

Recently, Parr, Szentpaly, and Liu[58] introduced the concept of electrophilicity index, ω, in terms of μ and η

$$\omega = \frac{\mu^2}{2\eta} \quad (15)$$

appraising the capacity of an electrophile to accept the maximal number of electrons in a neighboring reservoir of electron sea. We will profile these DFT conceptual indices as a function of the dihedral angle during the molecular internal rotation to examine their variation tendency.[50,53]

III. Computational Details

The above formulation has been implemented in the NWChem suite of software,[59] a publicly accessible, computational chemistry package from Pacific Northwest National Laboratory that is designed to run on high-performance parallel supercomputers and clusters. To test the implementation, we will at first investigate the dependences of the calculated rotational barrier height on the choice of basis sets and approximate exchange-correlation energy density functionals. The basis sets to be examined include Pople's[60,61] 6-31G, 6-31G*, 6-31G**, 6-31++G**, 6-311G*, and 6-311++G** and Dunning's[62] correlation consistent basis sets, cc-pVDZ, cc-pVTZ, aug-cc-pVDZ, and aug-cc-pVTZ. The approximate functionals considered are BeckHandH,[63] B3,[64] BLYP,[65,66] B3LYP,[66,67] X3LYP,[68] MPW1K,[69] Beck97GGA1,[70] Becke98,[71] HCTH-407p,[72] and TPSS,[73] covering most of the popular GGA, metaGGA, and hybrid forms of the exchange-correlation energy approximations currently available in the literature. For systematic calculations of the rotational barrier height for different dihedral angles, we use the B3LYP functional and Dunning's aug-cc-pVDZ basis set.

In regard to the rotational barrier height, there can be two categories, adiabatic (i.e., optimized geometry) and vertical (i.e., fixed geometry).[52,74–76] In the first case, both staggered and eclipsed conformers are in their respective optimized structure, whereas in the latter situation bond lengths and angles for the two conformers are fixed to be identical except for the changing dihedral angle. For the adiabatic series, each time the dihedral angle of the two conformers is altered, a geometrical optimization with the fixed dihedral angle will be performed for both conformers. For the vertical category, two cases are considered in this work. In the first case, we employ the optimized geometry of the staggered conformer as the starting structure and the eclipsed conformer is obtained from the starting structure by changing the dihedral angle from 180 to 0°. In the second case, we use the optimized eclipsed conformer as the reference and attain the staggered conformer by rotating the dihedral angle from 0 to 180°. For both vertical cases, no structural optimization is carried out. The dihedral angle considered for ethane is ∠H−C−C−H and for n-butane ∠C−C−C−C. For ethane, the dihedral angle change range was from 0 to 120° with the interval of 5°, whereas for *n*-butane, it was 0 to 180° with the interval of 10°. The tight self-consistent field convergence criterion and ultrafine integration grids are employed throughout. As a comparison, we also calculated the steric energy using natural bond orbitals for the two systems. The NBOFILE keyword in NWChem was used to create an input file to be used as the input for the stand-alone natural bond orbital analysis code, NBO 5.0.[77] In addition, profiles of DFT reactivity indices such as HOMO/LUMO, chemical potential, hardness, electrophilicity index, etc., relative to the eclipsed conformer are calculated for each dihedral angle with the help of eqs 12–15.

IV. Results and Discussion

Tables 1 and 2 show the total energy and its components from the two partition schemes, eqs 1 and 2, for the staggered and eclipsed conformations of ethane and *n*-butane, respectively. Also shown in the Tables are the adiabatic and vertical energy differences (eclipsed-staggered) between the two conformers for the two systems. As discussed in the above section, two vertical comparisons are possible, one using the staggered conformer

TABLE 1: The Total and Its Components in Two Decomposition Schemes, Eqs 1 and 2, for the Staggered and Eclipsed Conformers of Ethane at the B3LYP/aug-cc-pVDZ Level[a]

		C_2H_6 eclipsed (au)		eclipsed-staggered difference (kcal/mol)	
	C_2H_6 staggered (au)	optimized geometry	staggered geometry	adiabatic	vertical
T_s	78.99474	78.99274	79.01170	−1.25	10.64
J	80.03288	79.87268	80.05052	−100.52	11.07
E_x	−12.35102	−12.34889	−12.35297	1.34	−1.22
E_c	−0.71858	−0.71845	−0.71878	0.08	−0.12
V_{nn}	42.04320	41.87294	42.04889	−106.84	3.57
V_{ne}	−267.83850	−267.50391	−267.87201	209.95	−21.03
E	−79.83727	−79.83289	−79.83265	2.74	2.90
E_e	−145.76242	−145.75829	−145.77261	2.51	−6.39
E_q	1.82496	1.81806	1.84266	−4.26	11.11
E_s	64.10017	64.10734	64.09730	4.49	−1.80
HOMO	−0.34401	−0.34231	−0.34127	1.07	1.72
LUMO	−0.00775	−0.00737	−0.00747	0.24	0.18

[a] For the staggered conformation, the optimized structure was employed, but for the eclipsed conformer two geometrical structures were used, one from the structure optimization (adiabatic case) and the other from the staggered conformer (vertical case).

TABLE 2: The Total and Its Components in Two Decomposition Schemes, Eqs 1 and 2, for the Staggered and Eclipsed Conformers of *n*-Butane at the B3LYP/aug-cc-pVDZ Level[a]

		C_4H_{10} eclipsed (au)		eclipsed-staggered difference (kcal/mol)	
	C_4H_{10} staggered (au)	optimized geometry	staggered geometry	adiabatic	vertical
T_s	156.91140	156.90696	156.97832	−2.79	41.99
J	205.47614	207.28315	209.34708	1133.87	2428.96
E_x	−24.04670	−24.04593	−24.06138	0.48	−9.21
E_c	−1.38437	−1.38476	−1.38705	−0.24	−1.68
V_{nn}	130.10413	131.86906	133.92917	1107.47	2400.15
V_{ne}	−625.53394	−629.09314	−633.26758	−2233.35	−4852.75
E	−158.47333	−158.46466	−158.46146	5.44	7.45
E_e	−289.95367	−289.94092	−289.99133	8.00	−23.63
E_q	4.50441	4.49014	4.60665	−8.96	64.15
E_s	126.97592	126.98613	126.92324	6.41	−33.06
HOMO	−0.32326	−0.30874	−0.30582	9.11	10.95
LUMO	−0.00781	−0.01123	−0.01085	−2.15	−1.91

[a] For the staggered conformation, the optimized structure was employed, but for the eclipsed conformer two geometrical structures were used, one from the structure optimization (adiabatic case) and the other from the staggered conformer (vertical case).

as the reference and the other using the eclipsed structure for the purpose, but here as an illustration we tabulate only one case where the staggered geometry is employed because it possesses the lower total energy. It is seen that the total energy difference is similar in both adiabatic and vertical cases, 2.74 and 2.90 kcal/mol for ethane and 5.44 and 7.45 kcal/mol for *n*-butane, respectively. Even though the total energy differences are similar, the sign and magnitude of energy component differences in the two cases are vastly different for both of the two energy partition schemes, eqs 1 and 2, where one finds sign changes for ethane and drastic magnitude alteration for *n*-butane. As evidenced by the data in the two Tables, when the eclipsed conformer takes the structure of the staggered conformation, the fixed geometry facilitates quantum effects between the methyl/ethyl fragments, resulting in stronger electrostatic repulsion and smaller steric hindrance. The same is true for the fixed structure with the eclipsed conformation as will be seen in Figures 2 and 4 below.

Now let us look at the steric energy component for these species. With each conformer of ethane in the optimized geometry, the adiabatic difference of the steric energy difference gives 4.49 kcal/mol, indicating that the eclipsed conformer possessing a larger steric repulsion than the staggered conformer, consistent with the common sense of chemical intuition. This component is the dominantly positive contribution to make the total energy difference greater than zero. However, in the vertical cases where bond distance and angles take either the staggered or eclipsed values, the steric energy difference becomes negative, demonstrating that the eclipsed conformer acquires a less steric repulsion than the staggered counterpart. In this case, the dominant contributor changes to be the quantum effect ΔE_q with other two effects, electrostatic and steric, both negatively contributed. These observations are also valid for *n*-butane as seen from Table 2.

To have a flavor of how the local behavior of the steric energy density difference looks like for both the adiabatic and vertical cases, Figure 1 exhibits its three-dimensional distribution for ethane (Figure 1a) and *n*-butane (Figure 1b), respectively. For ethane, the adiabatic case is illustrated, whereas for *n*-butane the depicted difference is for the vertical comparison. The two structures have properly been aligned before the subtraction is made. It is observed that for ethane the red (positive) and green (negative) lobes near the right methyl group largely cancel each other and the net contribution is positive predominantly because of the red dots in the other part of the molecule. For the *n*-butane case where the vertical steric energy difference is negative (Table 2), we find from Figure 1b that contributions from the two methyl groups on the right portion of the molecule mostly cancel each other and it is mainly the green spots near carbons atoms that contribute to the overall negative value of the steric energy difference.

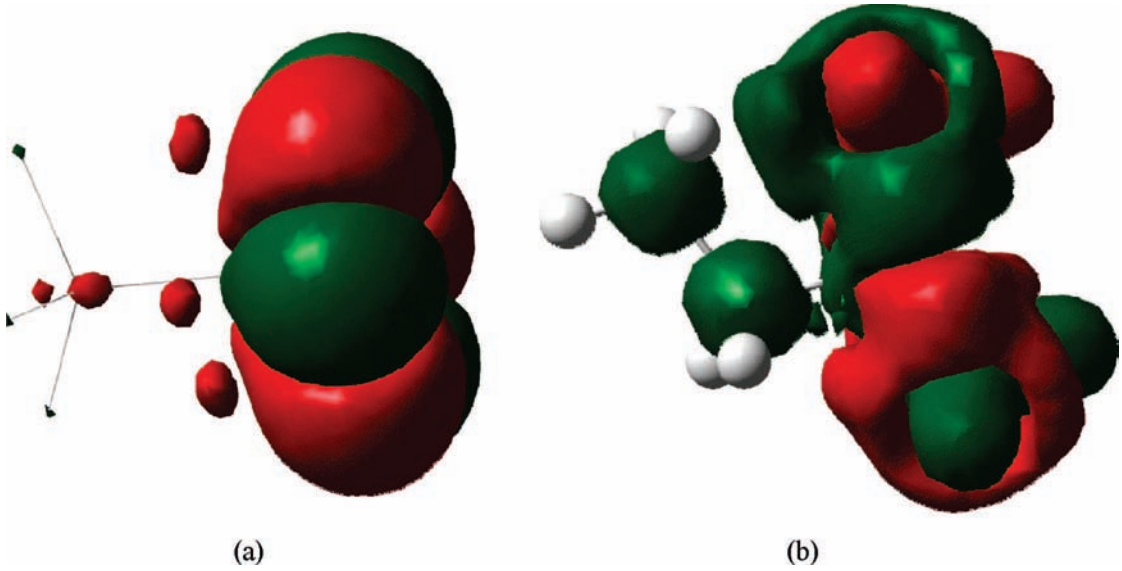

Figure 1. The contour map of the steric energy density difference at the value of ±0.005 (positive values in red and negative values in green) for (a) the eclipsed and staggered conformers of ethane and (b) the eclipsed and staggered conformers of *n*-butane. For ethane (a), the two conformers employ their respectively optimized structure. For *n*-butane (b), the staggered conformer uses its optimized structure but the eclipsed structure was obtained from the optimized staggered conformer by changing the ∠C−C−C−C dihedral angle from 180 to 0°. The structures of the two isomers were properly aligned before the steric energy densities are subtracted. GaussView was used in visualization.

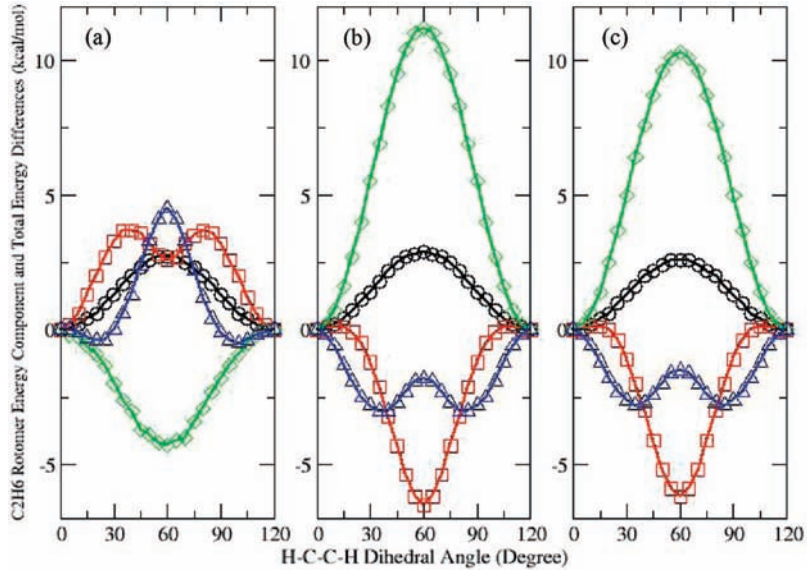

Figure 2. Differences of the total energy and energy components of eq 1 between the eclipsed and staggered conformers of ethane as a function of the dihedral angle. Three cases are considered here: (a) the two conformations employ their respectively optimized structure; (b) the eclipsed structure uses the optimized staggered structure (i.e., the eclipsed conformer is obtained the optimized staggered conformer by changing the ∠H−C−C−H dihedral angle from 180 to 0°); (c) the staggered structure is obtained from the optimized eclipsed structure by changing the dihedral change from 0 to 180°. Symbols are defined as follows. Circle, total energy difference; square, electrostatic; diamond, quantum; triangle, steric.

Next, we consider the impact of the basis set and approximate exchange-correlation energy density functional on energy components of the new energy partition scheme, whose results are shown in Tables 3 and 4, respectively. We find that among the 10 Pople and Dunning basis sets and 10 GGA/meta-GGA/hybrid functionals examined in this work, the dependence of the total energy difference on different choices of the basis set or functional is insignificant, varying at the range of about ±4% for each of the cases. More significant is that of the energy components, ranging from ±7.6 to 26.8% as shown from the STDEV values in Tables 3 and 4. The basis set dependence is twice as much as the functional dependence with the standard deviation percentage of about ±20 and 10%, respectively. Overall, the results are qualitatively consistent and no significant dependence of the new energy partition scheme on basis sets and functionals has been observed.

One of the main results of the present work is shown in Figure 2, where we examine the behavior of the energy difference of all quantities from the new energy partition scheme between the two conformers of ethane as a function of the dihedral angle changing from 0 to 120° with the interval of 5°. Three cases, one adiabatic and two vertical, are considered. Again, in the adiabatic case (Figure 2a), every structure of a different dihedral angle is fully optimized except for the dihedral angle held fixed, and the difference is taken between the eclipsed conformer and the optimized structure with the altered dihedral angle. In the two vertical

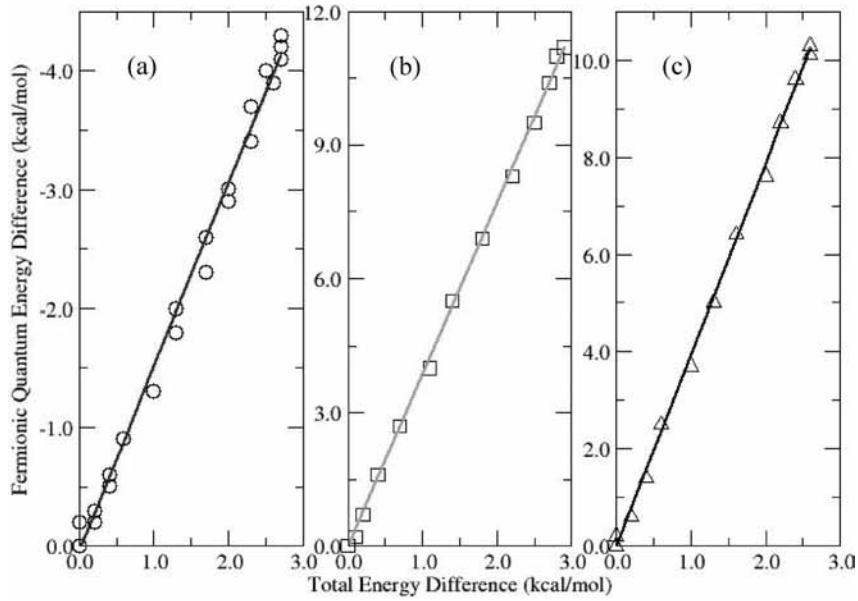

Figure 3. The strong linear correlation between the total energy difference ΔE and Fermionic quantum energy difference ΔE_q between the staggered and eclipsed conformers of ethane. The three cases are the same as Figure 1. Notice the *y* axis sign change from part a to parts b and c.

TABLE 3: Results of the Basis Set Dependency Test of the New Energy Partition Scheme in Eq 1 on the Energy Component Difference between the Eclipsed and Staggered Conformers of Ethane[a] (Units in kcal/mol)

basis set	ΔE_e	ΔE_q	ΔE_s	ΔE
6-31G	4.48	−7.47	5.66	2.67
6-31G*	5.05	−7.19	4.96	2.83
6-31G**	5.06	−6.70	4.44	2.80
6-31++G**	4.44	−6.40	4.71	2.75
6−311G*	3.76	−5.79	4.71	2.68
6−311++G**	3.74	−4.79	3.75	2.70
cc-pVDZ	5.02	−4.03	1.95	2.94
cc-pVTZ	5.42	−5.40	2.62	2.65
aug-cc-pVDZ	2.51	−4.26	4.49	2.74
aug-cc-pVTD	3.30	−4.87	4.20	2.63
std dev (%)	±21.7	±21.4	±26.8	±3.5

[a] The B3LYP functional was used.

TABLE 4: Results of the Exchange-Correlation Energy Density Functional Dependency Test of the New Energy Partition Scheme in Eq 1 on the Energy Component Difference between the Eclipsed and Staggered Conformers of Ethane[a] (Units in kcal/mol)

functional	ΔE_e	ΔE_q	ΔE_s	ΔE
BeckeHandH	2.72	−4.33	4.58	2.97
B3	2.60	−4.84	4.89	2.66
BLYP	2.11	−4.59	5.07	2.59
B3LYP	2.51	−4.26	4.49	2.74
X3LYP	2.52	−4.24	4.47	2.75
MPW1K	3.17	−4.06	3.84	2.95
Becke97GGA1	2.95	−4.47	4.29	2.77
Becke98	2.52	−4.37	4.59	2.75
HCTH407p	2.90	−4.19	4.00	2.71
metaGGA TPSS	3.00	−5.18	4.98	2.81
std dev (%)	±11.5	±7.6	±8.9	±4.2

[a] The aug-cc-pVDZ basis set was used.

cases, no structural optimization is carried out. Instead, in the first case of the vertical differences, Figure 2b, one employs the optimized structure of the staggered conformer and then alters the ∠H−C−C−H from 180° to the desired value, whereas in the second case, Figure 2c, the optimized eclipsed structure is utilized with the same dihedral angle modified from 0° to the target value between 0 to 120°. In agreement with what we have observed in the adiabatic and vertical differences from Tables 1 and 2, we discover from Figure 2 that the behavior of the total energy difference ΔE is similar in all cases, but the energy component differences are qualitatively different between the adiabatic and vertical cases. In specific, we find that in the adiabatic case, $\Delta E_q < 0$, $\Delta E_e > 0$ and $\Delta E_s > 0$, whereas in both of the vertical cases, they all change the sign, giving $\Delta E_q > 0$, $\Delta E_e < 0$ and $\Delta E_s < 0$.

Is it possible to find out from eq 1 which term is dominant in contributing to $\Delta E > 0$ in Figure 2, similar to what has been discussed elsewhere for other applications.[77,78] In parts b and c of Figure 2, since both ΔE_e and ΔE_s are negative, the only positive contribution is the quantum effect, ΔE_q, so it is secure to argue that ΔE_q is the dominant contributor. In Figure 2a, however, it is difficult to differentiate contributions from the two positive contributors, ΔE_e and ΔE_s, because they change their relative importance as the angle increases. Plotting ΔE_q vs ΔE, as shown in Figure 3, we find that there exists a remarkable linear relationship between these two quantities, indicating that the conformation change in all the three cases considered in this work is governed by the quantum effect. Notice however that there is a sign change for the *y* axis from part a of Figure 3 to parts b and c, suggesting that the correlation between ΔE_q and ΔE is positive for vertical cases and negative for the adiabatic difference. No other statistically significant correlation among other quantities has been discovered for ethane.

Shown in Figure 4 is another portion of the main results from this work, where, similar to Figure 2, behaviors of the quantities in eq 1 as a function of the *n*-butane's ∠C−C−C−C dihedral angle from 0 to 180° are exhibited. Consistent with Figure 2 as well as Tables 1 and 2, it is found that the adiabatic and two vertical cases give qualitatively different trends for these quantities. Different from Figure 2, it is seen that because of existence of hydrogen atoms whose orientations can be different at different dihedral angles, the behaviors of the quantities are more complicated. Also, the strong correlation between ΔE_q and ΔE for ethane disappears for *n*-butane, demonstrating that the linear relationship in

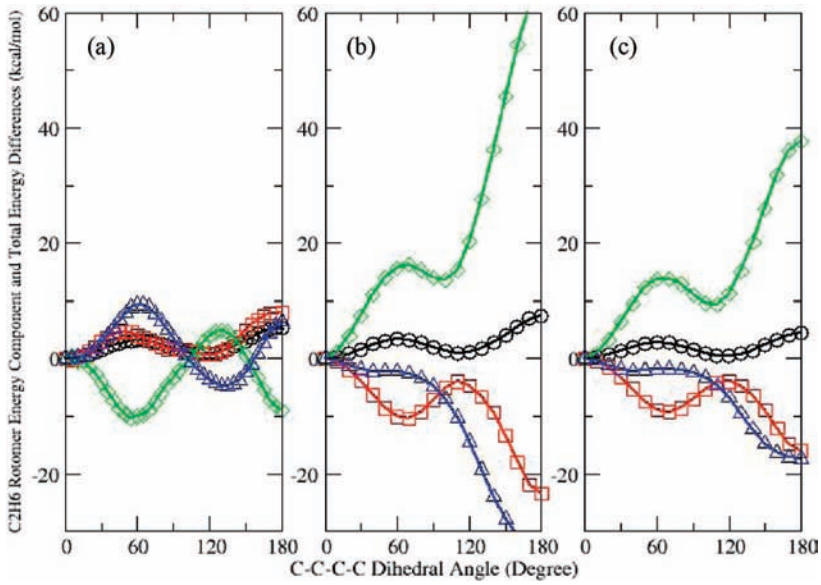

Figure 4. Differences of the total energy and energy components of eq 1 between the eclipsed and staggered conformers of n-butane as a function of the dihedral angle. Three cases are considered here: (a) the two conformations employ their respectively optimized structure; (b) the eclipsed structure uses the optimized staggered structure (i.e., the eclipsed conformer is obtained the optimized staggered conformer by changing the ∠C−C−C−C dihedral angle from 180 to 0°); (c) the staggered structure is obtained from the optimized eclipsed structure by changing the dihedral change from 0 to 180°. Symbols are defined as follows. Circle, total energy difference; square, electrostatic; diamond, quantum; triangle, steric.

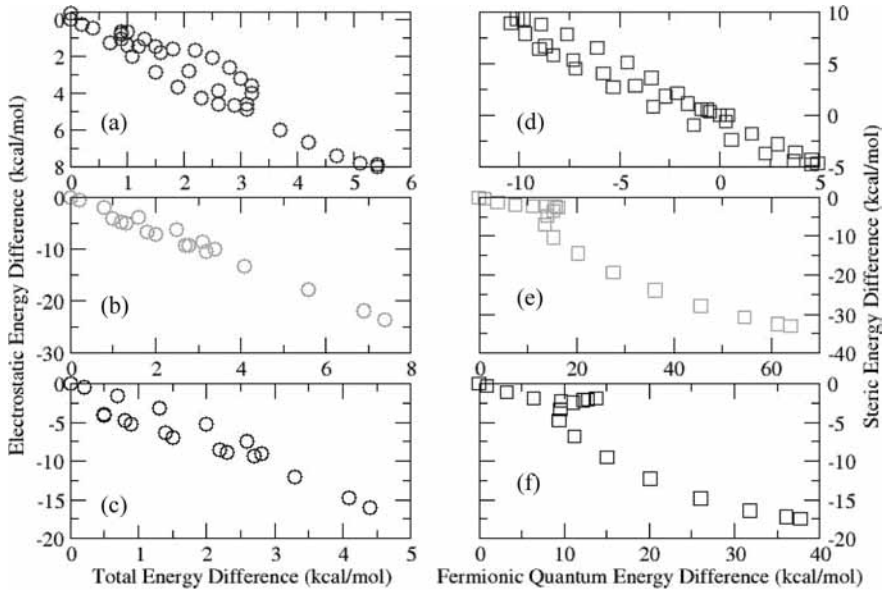

Figure 5. Weak correlations between ΔE and ΔE_e (left panel) and between ΔE_q and ΔE_s (right panel) between C_4H_{10} staggered and eclipsed conformers. An even weaker correlation between ΔE and ΔE_q was observed (not shown). Parts a−c and d−f represent the same three cases as in Figures 1–3.

Figure 3 is not universal. A couple of much weaker correlations, ΔE_e vs ΔE (parts a−c of Figure 5) and ΔE_q vs ΔE_s (parts d−f of Figure 5), for both the adiabatic and two vertical cases are displayed in Figure 5. Again, the correlations are weak and case dependent, evidencing that the relationships are not universal. An even weaker correlation between ΔE and ΔE_q has been discovered (not shown).

As a comparison, Figure 6 shows the results for the same three cases for *n*-butane as Figure 4 for the total and steric energy difference from another quantification of the steric effect available in the literature using natural bond orbitals. This definition uses the Fermi correlation from the Pauli Exclusion Principle as a measure of the steric effect, which in eq 1 has categorically been included in the fermionic quantum effect. Because of this fundamental difference in definition, it is no surprise to see from Figure 6 that there exists qualitative difference from what was observed in Figure 4 for the molecule. In particular, we find that in the adiabatic case, the steric energy difference from natural bond orbital (NBO) analysis in Figure 6 is almost always negative, suggesting that with their corresponding optimal structure the eclipsed conformer of *n*-butane possesses smaller steric repulsion than the staggered conformer. In the two vertical cases, however, the reverse becomes true. That is, the eclipsed conformer has a larger steric energy than the staggered conformer. These behaviors have also been observed in ethane (not shown). Though fundamentally different, these two quantifications of the steric effect both exhibit the paramount difference between the adiabatic and vertical differences, suggesting that the difference behavior of the

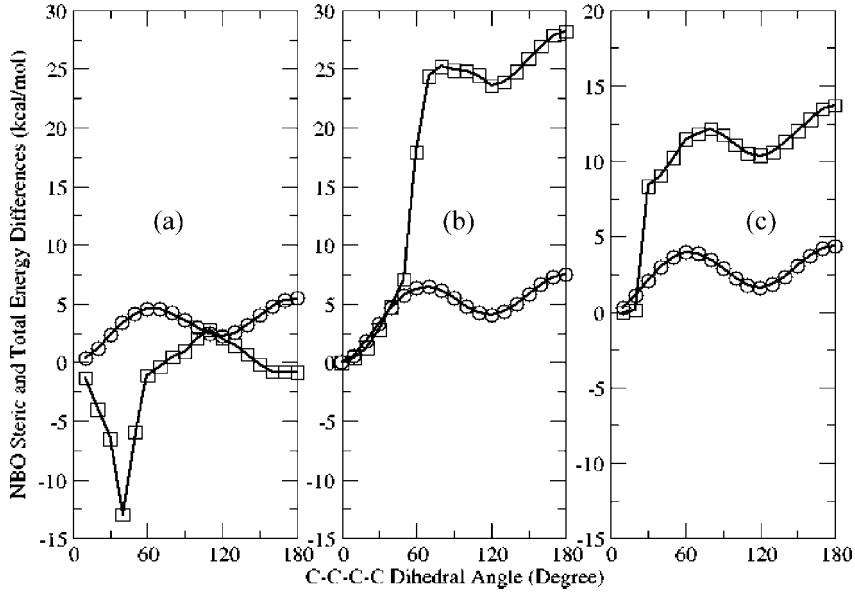

Figure 6. Differences of the total energy (circles) and the steric energy (squares) differences from the NBO analysis between the eclipsed and staggered conformers of ethane as a function of the dihedral angle. Three cases considered here include: (a) the two conformations take their respectively optimized structure; (b) the eclipsed structure employs the optimized staggered structure (i.e., the eclipsed conformer is obtained the optimized staggered conformer by changing the ∠C−C−C−C dihedral angle from 180 to 0°); (c) the staggered structure is obtained from the optimized eclipsed structure by changing the dihedral change from 0 to 180°.

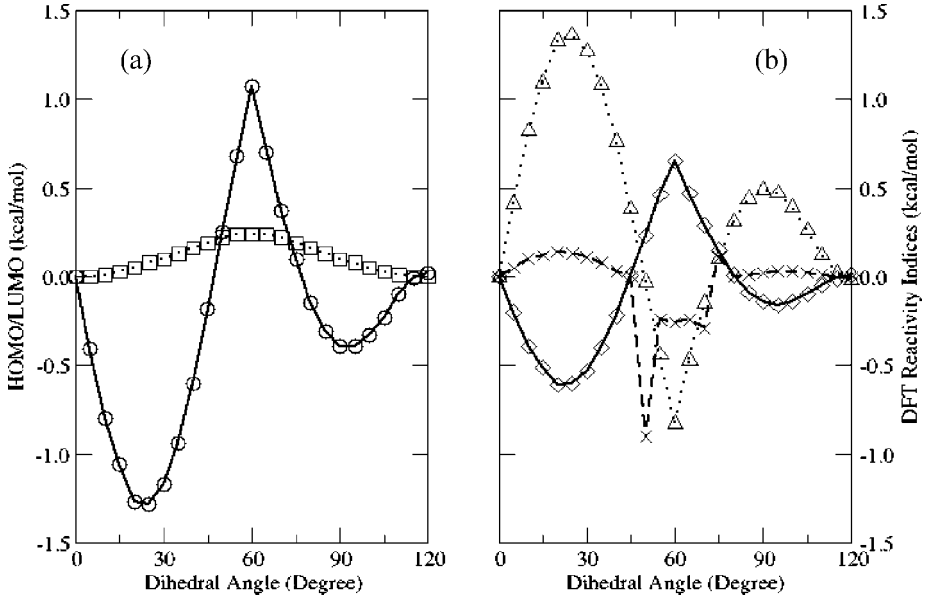

Figure 7. DFT reactivity index profiles (relative to the eclipsed conformer) as a function of the dihedral angle change from 0 to 120° for ethane: (a) HOMO (circle, solid line) and LUMO (square, dotted line); (b) chemical potential (diamond, solid line), hardness (triangle, dotted line), and electrophilicity index (cross, dashed line). Adiabatic structures have been employed.

two conformers in the adiabatic and vertical cases is qualitatively different from each other.

Finally, in Figure 7 as an example, we show the profiles of DFT reactivity indices as a function of the dihedral angle for ethane. Shown in Figure 7a are HOMO and LUMO profiles. As discovered earlier,[53,56] during the process of conformation changes, HOMO changes faster and fluctuates larger than LUMO does. This phenomenon is also observed in Figure 7a during the internal rotation process. In Figure 7b, chemical potential, hardness, and electrophilicity index (relative to the value of the eclipsed conformer) are obtained using eqs 12–15 for each of the ∠H−C−C−H dihedral angle. It is seen that from the eclipsed conformer to the staggered, chemical potential becomes smaller and hardness bigger, confirming that the maximum hardness principle comes into play. Also, the profile shapes of these two functions are dictated by the shape of the HOMO profile.[53,56] For the electrophilicity index profile in Figure 7b, consistent with earlier observations,[53,56] one finds that it is versatile, able to generate spikes of large amplitudes. We finally notice that our results in the Figure provide another manifestation for the so-called maximum hardness principle [78,79] and minimum electrophilicity principle.[80,81]

V. Concluding Remarks

On the basis of a new total energy partition scheme recently proposed by one of the authors, the nature of the internal rotational barrier height for the two conformers, staggered and eclipsed, of ethane and *n*-butane has systematically been

examined. The new quantification of the steric effect is density based and bears appealing characteristics such as exclusiveness, repulsiveness, extensiveness, as well as its intrinsic relationship with Bader's atoms in molecules approach. We considered the adiabatic and vertical differences where in the former the two conformers are in their respectively optimized structure, whereas in the latter fixed bond lengths and angles are employed. We found that, in the adiabatic case, the eclipsed conformer possesses a larger steric repulsion than the staggered conformer for both systems, which is consistent with the common sense of chemical intuition, but in the vertical cases the order is reversed with the staggered conformer retaining a larger steric repulsion. For ethane, a strong linear correlation between the total energy difference and the fermionic quantum energy difference has been discovered, indicating that the energy change as a function of the dihedral angle for ethane can quantitatively be determined by the quantum effect. This linear relationship, however, no longer holds for *n*-butane, whose behaviors in energy component differences has been found to be more complicated than ethane. The impact of basis set and density functional choices on the new energy partition scheme has been investigated, as has its comparison with another definition of the steric effect in the literature. No significant dependence of the new energy partition scheme on basis sets and approximate exchange-correlation energy functionals has been observed. Profiles of conceptual DFT reactivity indices such as HOMO/LUIMO, chemical potential, hardness, and electrophilicity index, as a function of dihedral angle changes have also been examined. Similar profile patterns to what were observed previously for other systems in conformation changes have also been detected in this study. Put together, these results suggest that the new energy partition scheme can provide in depth insights, complementary to other well established approaches in the literature, from a different perspective for the understanding of the origin of molecular internal rotation barriers, which appears to be rather complicated and system dependent.

Acknowledgment. The authors are grateful to Robert G. Parr and Lee Pedersen of University of North Carolina and Paul W. Ayers of McMaster University, Canada, for their valuable comments and suggestions. The work at Pacific Northwest National Laborartory (PNNL) was supported by the U.S. Department of Energy under Contract DE-AC06-76RLO 1830 (Office of Biological and Environmental Research, EMSL operations). The Pacific Northwest National Laboratory is operated by Battelle Memorial Institute. EMSL operations are supported by the DOE's Office of Biological and Environmental Research.

References and Notes

(1) Kemp, J. D.; Pitzer, K. S. *J. Chem. Phys.* **1936**, *4*, 749.
(2) Mulliken, R. S. *J. Chem. Phys.* **1939**, *7*, 339.
(3) Pitzer, R. M.; Lipscomb, W. N. *J. Chem. Phys.* **1963**, *39*, 1995.
(4) Wyatt, R. E.; Parr, R. G. *J. Chem. Phys.* **1964**, *41*, 3262.
(5) Clementi, E.; Davis, D. R. *J. Chem. Phys.* **1966**, *45*, 2593.
(6) Alexande, M. H. J. *Chem. Phys.* **1967**, *47*, 2423.
(7) Sovers, O. J.; Kern, C. W.; Pitzer, R. M.; Karplus, M. *J. Chem. Phys.* **1968**, *49*, 2592.
(8) Epstein, I. R.; Lipscomb, W. N. *J. Am. Chem. Soc.* **1970**, *92*, 6094.
(9) England, W.; Gordon, M. S. *J. Am. Chem. Soc.* **1971**, *93*, 4649.
(10) Lowe, J. P. *Science* **1973**, *179*, 527.
(11) Christiansen, P. A.; Palke, W. E. *Chem. Phys. Lett.* **1975**, *31*, 462.
(12) Payne, P. W.; Allen, L. C. Barriers to rotation and inversion. In *Modern Theoretical Chemistry*; Schaefer, H. F., III, Ed.; Plenum Press: New York and London, 1977; Vol. 4, pp 29−108.
(13) Brunck, T. K.; Weinhold, F. *J. Am. Chem. Soc.* **1979**, *101*, 1700.
(14) Pitzer, R. M. *Acc. Chem. Res.* **1983**, *16*, 207.
(15) Bader, R. F. W.; Cheeseman, J. R.; Laidig, K. E.; Wiberg, K. B.; Breneman, C. *J. Am. Chem. Soc.* **1990**, *112*, 6530.
(16) Reed, A. E.; Weinhold, F. *Isr. J. Chem.* **1991**, *31*, 277.
(17) Wiberg, K. B. Rotation barriers: Ab initio computations. In *Encyclopedia of Computational Chemistry*; Schelyer, P. v. R., Ed.; John Wiley & Sons: Berlin, 1998; pp 2518−2525.
(18) Goodman, L.; Gu, H. *J. Chem. Phys.* **1998**, *109*, 72.
(19) Goodman, L.; Gu, H.; Pophristic, V. *J. Chem. Phys.* **1999**, *110*, 4268.
(20) Goodman, L.; Pophristic, V.; Weinhold, F. *Acc. Chem. Res.* **1999**, *32*, 983.
(21) Pophristic, V.; Goodman, L. *Nature* **2001**, *411*, 565.
(22) Schreiner, P. R. *Angew. Chem., Int. Ed.* **2002**, *41*, 3579–3581.
(23) Bickelhaupt, F. M.; Baerends, E. J. *Angew. Chem., Int. Ed.* **2003**, *42*, 4183.
(24) Weinhold, F. *Angew. Chem., Int. Ed.* **2003**, *42*, 4188.
(25) Mo, Y.; Wu, W.; Song, L.; Lin, M.; Zhang, Q.; Gao, J. *Angew. Chem., Int. Ed.* **2004**, *43*, 1986.
(26) Bohn, R. K. *J. Phys. Chem. A* **2004**, *108*, 6814.
(27) Song, L.; Lin, Y.; Wu, W.; Zhang, Q.; Mo, Y. *J. Phys. Chem. A* **2005**, *109*, 2310.
(28) Fernandez, I.; Frenking, G. *Chem.−Eur. J.* **2006**, *12*, 3617.
(29) Mo, Y.; Gao, J. *Acc. Chem. Res.* **2007**, *40*, 113.
(30) Parr, R. G.; Ayers, P. W.; Nalewajski, R. F. *J. Phys. Chem. A* **2005**, *109*, 3957.
(31) Frenking, G.; Krapp, A. *J. Comput. Chem.* **2007**, *28*, 15.
(32) Hoffmann, R. *THEOCHEM* **1998**, *424*, 1.
(33) Weisskopf, V. F. *Science* **1975**, *187*, 605.
(34) Badenhoop, J. K.; Weinhold, F. *J. Chem. Phys.* **1997**, *107*, 5406.
(35) Luken, W. L.; Beratan, D. N. *Theor. Chem. Acc.* **1982**, *61*, 1432.
(36) Liu, S. B. *J. Chem. Phys.* **2007**, *126*, 244103.
(37) Bader, R. F. W. *Atoms in Molecules - A Quantum Theory*; Oxford University Press: Oxford, 1990.
(38) Parr, R. G.; Yang, W. *Density Functional Theory of Atoms and Molecules*; Oxford University Press: Oxford, 1989.
(39) March, N. H. *Phys. Lett. A* **1986**, *113*, 476.
(40) Levy, M.; Ou-Yang, H. *Phys. Rev. A* **1988**, *38*, 625.
(41) Herring, C.; Chopra, M. *Phys. Rev. A* **1988**, *37*, 31.
(42) Savin, A.; Becke, A. D.; Flad, J.; Nesper, R.; Preuss, H.; von Schnering, H. G. *Angew. Chem., Int. Ed.* **1991**, *30*, 409.
(43) Holas, A.; March, N. H. *Phys. Rev. A* **1991**, *44*, 5521.
(44) von Weizsäcker, C. F. *Z. Phys.* **1935**, *96*, 431.
(45) Nagy, A. *Chem. Phys. Lett.* **2007**, *449*, 212.
(46) Liu, S. B. *J. Chem. Phys.* **2007**, *126*, 191107.
(47) Fisher, R. A. *Proc. Cambridge Philos. Soc.* **1925**, *22*, 700.
(48) Nagy, A.; Liu, S. B. *Phys. Lett. A* **2008**, *372*, 1654.
(49) Geerlings, P.; De Proft, F.; Langenaeker, W. *Chem. Rev.* **2003**, *103*, 1793.
(50) Liu, S. B. *J. Chem. Sci.* **2005**, *117*, 477.
(51) Fan, W. J.; Zhang, R. Q.; Liu, S. B. *J. Comput. Chem.* **2007**, *28*, 967.
(52) Rong, C.; Lian, S.; Yin, D.; Zhong, A. G.; Zhang, R. Q.; Liu, S. B. *Chem. Phys. Lett.* **2007**, *434*, 149.
(53) Zhong, A. G.; Rong, C.; Liu, S. B. *J. Phys. Chem. A* **2007**, *111*, 3132.
(54) Huang, Y.; Zhong, A. G.; Rong, C.; Xiao, X. M.; Liu, S. B. *J. Phys. Chem. A* **2008**, *112*, 305.
(55) (a) Iczkowski, R. P.; Margrave, J. L. *J. Am. Chem. Soc.* **1961**, *83*, 3547. (b) Parr, R. G.; Donnelly, R. A.; Levy, M.; Palke, W. E. *J. Chem. Phys.* **1978**, *68*, 3801.
(56) Mulliken, R. S. *J. Chem. Phys.* **1934**, *2*, 782.
(57) Parr, R. G.; Pearson, R. G. *J. Am. Chem. Soc.* **1983**, *105*, 7512.
(58) (a) Parr, R. G.; Szentpaly, L. V.; Liu, S. B. *J. Am. Chem. Soc.* **1999**, *105*, 1922. (b) For a review, see Chattaraj, P. K.; Sarkar, U.; Roy, D. R. *Chem. Rev.* **2006**, *106*, 2065.
(59) Aprà, E. NWChem. *A computational chemistry package for parallel computers version 5.0*; Pacific Northwest National Laboratory: Richland, Washington 99352-0999, USA, 2005.
(60) Hariharan, P. C.; Pople, J. A. *Theor. Chim. Acta* **1973**, *28*, 213.
(61) Francl, M. M.; Pietro, W. J.; Henre, W. J.; Binkley, J. S.; Gordon, M. S.; DeFrees, D. J.; Pople, J. A. *J. Chem. Phys.* **1982**, *77*, 3654.
(62) Dunning, T. H., Jr. *J. Chem. Phys.* **1989**, *90*, 1007.
(63) Becke, A. D. *J. Chem. Phys.* **1992**, *98*, 1372.
(64) XC slater 0.8 becke88 nonlocal 0.72 HFexch 0.2
(65) Becke, A. D. *Phys. Rev. A* **1988**, *38*, 3098.
(66) Lee, C.; Yang, W.; Parr, R. G. *Phys. Rev. B* **1988**, *37*, 785.
(67) Becke, A. D. *J. Chem. Phys.* **1993**, *98*, 5648.
(68) Xu, X.; Goddard, W. A. *Proc. Natl. Acad. Sci. USA* **2004**, *101*, 2673.
(69) Lynch, B. J.; Fast, P. L.; Harris, M.; Truhlar, D. G. *J. Phys. Chem. A* **2000**, *104*, 4811.
(70) Cohen, A. J.; Handy, N. C. *Chem. Phys. Lett.* **2000**, *316*, 160.

(71) Schmider, H. L.; Becke, A. D. *J. Chem. Phys.* **1998**, *108*, 9624.
(72) Boese, A. D.; Chandra, A.; Martin, J. M. L.; Marx, D. *J. Chem. Phys.* **2003**, *119*, 5965.
(73) Tao, J. M.; Perdew, J. P.; Staroverov, V. N.; Scuseria, G. E. *Phys. Rev. Lett.* **2003**, *91*, 146401.
(74) Liu, S. B.; Langenaeker, W. *Theor. Chem. Acc.* **2003**, *110*, 338.
(75) Zhong, A. G.; Liu, S. B. *J. Theor. Comput. Chem.* **2005**, *4*, 833.
(76) Rong, C.; Lian, S.; Yin, D.; Shen, B.; Zhong, A. G.; Bartolotti, L.; Liu, S. B. *J. Chem. Phys.* **2006**, *125*, 174102.
(77) Glendening, E. D.; Badenhoop, J. K.; Reed, A. E.; Carpenter, J. E.; Bohmann, J. A.; Morales, C. M.; Weinhold, F. ;Theoretical Chemistry Institute: University of Wisconsin, Madison, 2001.
(78) Pearson, R. G. *J. Chem. Educ.* **1999**, *76*, 267.
(79) Parr, R. G.; Chattaraj, P. K. *J. Am. Chem. Soc.* **1991**, *113*, 1854.
(80) Noorizadeh, S. *J. Phys. Org. Chem.* **2007**, *20*, 514.
(81) Chattaraj, P. K.; Giri, S. *J. Phys. Chem. A* **2007**, *111*, 11116.

JP800376A